



LAWRENCE
LIVERMORE
NATIONAL
LABORATORY

Ion Separation Effects in Mixed-Species Ablator and Fuels for Inertial Confinement Fusion Implosions

P. Amendt, C. Bellei, J. S. Ross, J. Salmonson, S.
Wilks

June 26, 2013

European Physical Society
Espoo, Finland
July 1, 2013 through July 5, 2013

Disclaimer

This document was prepared as an account of work sponsored by an agency of the United States government. Neither the United States government nor Lawrence Livermore National Security, LLC, nor any of their employees makes any warranty, expressed or implied, or assumes any legal liability or responsibility for the accuracy, completeness, or usefulness of any information, apparatus, product, or process disclosed, or represents that its use would not infringe privately owned rights. Reference herein to any specific commercial product, process, or service by trade name, trademark, manufacturer, or otherwise does not necessarily constitute or imply its endorsement, recommendation, or favoring by the United States government or Lawrence Livermore National Security, LLC. The views and opinions of authors expressed herein do not necessarily state or reflect those of the United States government or Lawrence Livermore National Security, LLC, and shall not be used for advertising or product endorsement purposes.

Ion Separation Effects in Mixed-Species Ablators and Fuels for Inertial Confinement Fusion Implosions

Peter Amendt, Claudio Bellei, J. Steven Ross, Jay Salmonson and Scott Wilks

Lawrence Livermore National Laboratory, Livermore CA 94551 USA

E-mail: amendt1@llnl.gov

Abstract. Current efforts to demonstrate ignition on the National Ignition Facility are focused on the use of plastic (CH) ablaters. Mainline simulation techniques for modeling CH capsule implosions treat the ablator as an average atom fluid and neglect potential species separation phenomena. The x ray-driven mass-ablation process for a mixture is shown to lead to significant species separation, parasitic energy loss according to thermodynamic arguments, and reduced rocket efficiency. The phenomenon of species separation potentially applies to mixed-species thermonuclear fuels such as D³He and DT with an attendant energy expense.

PACS numbers: 52.57.-z, 52.57.Bc, 52.38.Ph

1. Introduction

Efforts to demonstrate thermonuclear breakeven and ignition on the National Ignition Facility (NIF) continue in earnest [1]. A plastic (CH) capsule ablator absorbs soft x rays generated in a high-Z cylindrical enclosure (or hohlraum) that is heated by nearly 1.5 MJ of 0.351 μm laser light. In direct reaction to the x ray-driven ablation, the remainder of the shell inwardly accelerates and compresses an encapsulated deuterium (D) and tritium (T) fuel mixture to thermonuclear conditions.

Experiments on the NIF dedicated to measuring the peak implosion speed of the imploding shell with x-ray backlighting techniques have consistently shown a $10\pm 5\%$ deficit compared with radiation-hydrodynamic (RH) simulation predictions [2]. Explanations for this discrepancy range from equation-of-state uncertainties for CH, higher-than-expected x-ray albedo of the CH ablator, to reduced hohlraum coupling to the capsule from anomalous laser backscatter phenomena. If a reduced coupling efficiency is responsible for the observed shortfall in peak implosion speed of $5\pm 5\%$ relative to what is required for ignition ($\sim 370 \mu\text{m/ns}$), the expectation is that this deficit can be overcome with higher laser powers ($\sim 500 \text{ TW}$) and the use of depleted uranium hohlraums. Indeed, a recent high power (520 TW) and energy (1.86 MJ) shot with a uranium hohlraum appears to have demonstrated the required peak implosion velocity and remaining ablator mass above the ignition goal [3]. However, multi-ion species capsules may cause separation phenomena that motivate the use of potentially more efficient ablator materials such as high-density carbon (HDC) - which is just starting to be explored on the NIF.

An often-overlooked physical phenomenon in inertial confinement fusion (ICF) is the potential for species separation from acceleration-induced pressure gradients and self-generated electric fields. In the case of CH ablators, the large ion mass ratio of carbon to hydrogen (~ 12) allows the possibility of barodiffusion-driven species separation [4-8]. Similarly, the significant difference in charge-to-mass ratios for (fully ionized) C and H may allow electrodiffusion-mediated species separation to occur as well [5-8]. Under warm-dense matter conditions as in an ablation front, diffusive time scales are often long relative to an implosion time scale, but strong pressure gradients and electric fields ($>10^4$ statVolts/cm) can still drive an appreciable separation of species occurring well within an implosion time [5]. This physical feature is analogous to the species segregation that takes place in the upper atmosphere above the turbopause where the standard barometric formula corrected for buoyancy applies [9].

In this article thermodynamic arguments are used to show that an ablating mixed-species shell leads to an energy loss in the process of separating the constituent ions. This result is consistent with a calculated reduction in rocket ablation efficiency. Direct evidence for significant species separation is known based on Thomson scattering measurements of a direct-drive CH_2 planar sample [10]. The main conclusion of this work is that mainline (single) fluid-based simulation techniques used in ICF studies currently neglect species separation phenomena, thereby motivating adaptations of these standard RH tools, use of multi-fluid particle-in-cell (PIC) simulation techniques [11], or the simplifying option of single-species ablators.

Some physical insight into why average-atom RH simulations may overestimate (areal) mass ablation rates in a mixed species ablator can be gained as follows. Consider a dissociated pair of C and H atoms, each borne with an average thermal energy of $3k_B T / 2$ and converted into radially directed kinetic energy $m_j v_j^2 / 2$ at the ablation front, where k_B is Boltzmann's constant, T is the temperature, and the species label $j=C$ or H. If each atom is allowed to move at its own separate velocity, the momentum for this pair of atoms follows as $p_{sep} = m_H v_H + m_C v_C = \sqrt{3k_B T} \cdot (\sqrt{m_H} + \sqrt{m_C})$. On the other hand, RH simulations force the H and C atoms to move together in an average-atom sense such that $3k_B T = (m_H + m_C) \cdot \bar{v}^2 / 2$, where \bar{v} is the average fluid speed. Upon forming the resulting momentum for this average atom, we have $p_{RH} = (m_H + m_C) \bar{v} = \sqrt{6k_B T(m_H + m_C)}$. Forming the ratio of the two momenta gives $p_{RH} / p_{sep} = \sqrt{2(m_H + m_C)} / (\sqrt{m_H} + \sqrt{m_C})$, which equals 1.1422. By not allowing the H and C atoms to physically separate, the RH simulation tools may be overestimating the mass ablation rate by nearly 14% according to this argument.

The CH ablator used in ignition studies on the NIF to date have contained buried mid-Z dopant layers as well, e.g., 1.0 at.% Ge or 2.0 at.% Si, to control x-ray preheat of the interior DT fuel [12]. Adapting the above argument to the case of 1.0 at.% Ge in CH shows that RH codes may overestimate the momentum transferred to the shell from ablating $\text{CH}_{0.98}\text{Ge}_{0.02}$ by over 16%.

An ablating ICF shell is necessarily in a plasma state, and modifications to the above arguments are required. Accordingly, we start with a rocket model for the ablating shell: $M\dot{v} = -v_E\dot{M}$, where M is the remaining shell mass, \dot{v} is the shell acceleration, and $v_E = 2\sqrt{(Z+1)k_B T / Am_H}$ is the exhaust speed [13], Z is the ionization state of the ablated ion and A its atomic mass number. For a composite ablator material or mixture, e.g., CH, we form the mass-weighted exhaust speed $\bar{v}_E = \alpha v_{E,1} + (1-\alpha)v_{E,2}$, where α is the ratio of light-ion mass density to the total mass density. The rocket efficiency η is defined as the ratio of shell kinetic energy to the exhaust energy:

$$\eta = \frac{E_{kin}}{E_{ex}} = \frac{M [\ln(M / M_0)]^2}{(M_0 - M)} \cdot \left\{ \frac{(\alpha v_{E,1} + (1-\alpha)v_{E,2})^2}{\alpha v_{E,1}^2 + (1-\alpha)v_{E,2}^2} \right\}, \quad (1)$$

where M_0 is the initial shell mass. The expression in braces in Eq. (1) describes the change in rocket efficiency due to multi-species effects. Figure 1 depicts the rocket efficiency decrease in a CH ablator as a function of hydrogen number fraction and the possible ionization states of carbon. In indirect-drive implosions the ionization state of carbon near the head of the ablation front is in the range of 4-to-5, giving a nearly 6-8% decrease in rocket efficiency for CH compared with a pure species ablator. A further decrease in rocket efficiency is predicted for doped ablators as well. Generalizing Eq. (1) to three species for a 1.0 at.% Ge doping of CH shows that the rocket efficiency is further degraded, ranging from 9.4% (8.2%) for $Z_{Ge}=9$ and $Z_C=4$ (5).

RH simulations with alternating layers of pure C and H can be used to assess the impact of an *imposed* species separation on the average hydrodynamics of an ablatively-driven implosion (but without inter-species penetration). By imposing the constraints of equal areal mass density: $\rho_H \Delta_H + \rho_C \Delta_C = \rho_{CH} (\Delta_H + \Delta_C)$, and equal areal atomic number density: $n_H \Delta_H = n_C \Delta_C$, the prescribed relative layer thicknesses and mass densities are derived:

$$\frac{\Delta_C}{\Delta_H} = \frac{A_C \rho_{CH} / \rho_C}{1 + A_C (1 - \rho_{CH} / \rho_C)}, \quad (2a)$$

$$\frac{\rho_H}{\rho_C} = 1 + \frac{\Delta_C}{\Delta_H} \left(1 - \frac{\rho_C}{\rho_{CH}} \right), \quad (2b)$$

where $\Delta_H(\Delta_C)$ is the thickness of the hydrogen (carbon) layer, $\rho_H(\rho_C)$ is the mass density of the hydrogen (carbon) layer, $n_H(n_C)$ is the number density of the hydrogen (carbon) layer, and A_C is the atomic weight of carbon. The mass density of CH is chosen as 1.05 g/cc, and the density of the graphite (an allotrope of carbon) $\rho_C=2.2\text{g/cc}$. Figure 2 shows that the average hydrodynamics is hardly affected by separation, but energy must be expended to realize such a configuration, which we now estimate.

The energy expended in segregating an initially homogeneous plasma mixture follows from thermodynamic arguments. It is well known that energy must be invested to change the concentration of a solution by reducing or removing the solvent [9], and the same principle carries over to driven species separation in an ablating plasma. For this purpose, the thermodynamic potential Ξ (or Legendre transform of the energy with respect to entropy and volume) is the most suitable starting point. Figure 3 shows schematically two configurations of a CH mixture, and we calculate the change in thermodynamic potential $\Delta\Xi$ from an initially mixed state (left) to a partially segregated one (right), assuming constant temperature and pressure conditions and ideal gas behaviour:

$$\begin{aligned} \Delta\Xi[kJ] = 4.0 [N_i / 5 \cdot 10^{20}] T[eV] \cdot \{ & 2c \ln [c / (1-c)] + 2 \ln (1-c) - (1+Z_C - c\Delta Z) \ln (1+Z_C - c\Delta Z) + \\ & (Z_C - c\Delta Z) \ln (Z_C - c\Delta Z) - (1+Z_H + c\Delta Z) \ln (1+Z_H + c\Delta Z) + (Z_H + c\Delta Z) \ln (Z_H + c\Delta Z) + \\ & (2+Z_C + Z_H) \ln (2+Z_C + Z_H) - (Z_C + Z_H) \ln (Z_C + Z_H) \}, \end{aligned} \quad (3)$$

where N_i is the number of ablator ions, c is the number fraction of H ions, and $\Delta Z = Z_C - Z_H$. Figure 4 shows the separation energy as a function of hydrogen concentration for $Z_H=1$ and several values of Z_C at 300 eV [14], indicating a significant amount of energy particularly if the ion separation is nearly complete. NIF experiments consistently show a nearly 15% deficit in (inferred) absorbed capsule energy compared with the nominal level of ~ 170 kJ [15], allowing for a possible role of separation energy losses. By comparison, direct-drive implosions are much less susceptible to this separation energy loss, owing to the relatively fewer number of ablator ions (due to the low ablation speed) and the high laser coupling efficiency to the capsule ($\sim 60\%$).

Appreciable species separation can be driven by pressure gradients, electric fields and temperature gradients, provided collisional slowing of the ions is not prohibitively large. To

assess the degree of species separation in an ICF implosion, we consider the steady-state momentum balance for H and C ions, coupled with mass conservation:

$$v_H v'_H = -P'_H / \alpha \rho + Z_H e E / m_H - v_{HC} (v_H - v) / (1 - \alpha), \quad (4a)$$

$$v v' = -P' / \rho, \quad (4b)$$

$$v'_H - v' = -(v_H - v) [\rho' / \rho + 2 / r] - v_H \alpha' / \alpha, \quad (4c)$$

where primes denote the spatial derivative, P_H is the hydrogen pressure, ρ is the total mass density, v_{HC} is the hydrogen-carbon collision frequency, P is the total pressure, $v \equiv \alpha v_H + (1 - \alpha) v_C$ is the mass-weighted fluid speed, and r is the spherical radial coordinate. Combining Eqs. 4(a-b), transforming to the (local) moving frame of the mean fluid ($v = 0$), and using $E = (k_B T / e) \{-P' / P + \alpha' / D [(1 - \alpha) Z_C + \alpha Z_H m_C / m_H]\}$ [5], we find:

$$\alpha' = \frac{v_H \left(v' + v'_H + \frac{v_{HC}}{1 - \alpha} \right) D^2 - \frac{P'}{\rho} (D^2 - D(1 + Z_H))}{\frac{P}{\rho} \left[\frac{Z_H \Delta Z}{((1 - \alpha) Z_C + \alpha Z_H m_C / m_H)} - (1 + Z_H) m_H / m_C \alpha \right]}, \quad (5)$$

where $D \equiv \alpha(1 + Z_H) + (1 - \alpha)(1 + Z_C) m_H / m_C$, and the usual plasma barometric formula [$\alpha' = k_\alpha(\alpha; Z_H, Z_C, m_H, m_C) \cdot P' / P$] is recovered in the limit of $v_H = 0$ [5]. Figure 5 shows application of Eqs. (4c, 5) to an ignition-scale RH simulated capsule implosion just after 4th shock launch. The leading edge of the ablation front is defined as $P' = 0$, giving $\alpha' = 0$ to zeroth order in v_H . Strong species separation is predicted, giving a carbon-rich plasma persisting for nearly 1mm behind the ablation front, and a distinctly hydrogen-rich region extending to larger radii. Although most of the steady-state separation occurs well outside the sonic horizon and cannot directly influence the ablation process, the predicted separation configuration requires an energy expense according to Eq. 3 that derives from establishing locally lower entropy. Within the sonic point, transient separation can occur due to the difference in mean free paths for a large-angle scattering event between an ablating hydrogen and carbon ion: $\lambda_{HC} / \lambda_{CC} \approx Z_C^2 \sqrt{(1 + A_c) / 2A_c} \gg 1$.

A further consequence of species separation in the ablator is the potential for differential x-ray absorption in a converging geometry. Consider two contiguous spherical shells of thickness

Δr and inner radius r_0 of the interior (carbon-rich) shell. Using that the areal mass ablation rate \dot{m} scales as the incident x-ray flux to the $3/4$ power [16] and neglecting the opacity of the hydrogen in the shells, we obtain for the differential change in areal mass ablation rate from the combined effects of spherical geometry and species separation:

$$\frac{\delta\dot{m}}{\dot{m}} = -\frac{3}{4}\left(\frac{\Delta}{r_0}\right)^2\left(1 + \frac{\Delta}{r_0}\right)(2c-1), \quad (6)$$

where c is the hydrogen fraction in the outer shell. Thus, a reduced x-ray flux at the ablation front ($r=r_0$) arises from a surplus of carbon in the adjacent spherical layer. For a shell aspect ratio $r_0/\Delta=3$ and $c=0.8$, the fractional loss in areal mass ablation rate is $\approx 6.7\%$. This reduced ablation rate translates into a deficit of peak implosion speed v_{imp} of nearly 2%, using the scaling relation: $v_{imp} \approx \dot{m}^{0.3}$ [16].

There is recent experimental evidence for significant species separation in CH_2 planar foils fielded on the Omega Laser Facility [17], according to Thomson scattering measurements of collective electron-plasma and ion-acoustic fluctuations [10]. The CH_2 foil is directly heated with 10 laser beams with 5kJ total energy at 3ω (0.35 μm wavelength), and Thomson scattering is measured 4 mm from the foil surface using a 30J 2ω probe laser with a 1 ns pulse length. Using a series of target shots the plasma evolution is measured from 2.5 ns to 9 ns after the rise of the heater beams. Measuring the electron density and temperature from the electron-plasma fluctuations constrains the fit of the two-ion species theoretical form factor [18] for the ion feature such that the ion temperature, plasma flow velocity and ion species fraction are determined. The ion species fraction is determined to an accuracy of $\pm 6\%$. Figure 6 shows the inferred species fraction history with a significant hydrogen fraction persisting beyond 6 ns before the ablated carbon starts to appreciably enter the Thomson scattering volume. This is believed to be the first direct evidence of species separation in an ICF-relevant experiment.

The phenomenon of species separation also has implications for thermonuclear mixed-species equimolar fuels such as D^3He and DT . Similar to the case of a mixed-species ablator the presence of electric fields and pressure gradients may overcome collisional drag to transiently separate the two ion species and lower the entropy, resulting in a sink of energy. In the case of an ICF fuel the strong gradients responsible for species separation may arise within the shock fronts that transit the fuel. Although the separation is only transient, energy must be invested to realize the associated reduced entropy and is ultimately manifested as thermal heating upon (diffusive)

remixing following shock passage. Figure 7 shows the calculated separation energy from the thermodynamic potential, cf., Eq. (3), for a NIF-scale implosion where the total energy delivered to the DT fuel up to ignition onset is in the range of 10-12 kJ based on RH simulations. Depending on the average degree of separation at ignition of the central hot spot (~ 10 keV) when the mass-weighted fuel ion temperature is ~ 1 keV, significant kinetic energy may be converted to undesired thermal energy. Recent experiments on the Omega laser facility with DT fuels show anomalously high TT neutron reactions compared with RH simulations, which could be indicative of fuel species stratification where T ions preferentially populate the centre of the fuel [19]. The above thermodynamic argument must be tempered by the fact that a central-hot spot implosion is intrinsically isobaric and not isothermal, the potential roles of viscosity and turbulence in separation are not considered here, and acoustic time scales need to be sufficient to allow a physical separation of species across a significant fraction of a fuel radius.

The rate of entropy generation (per unit volume) \dot{s} associated with post-shock diffusive re-mixing in the main DT fuel layer from multiple shock transits can be estimated from the expression $\dot{s} = -i_D \cdot \nabla \mu / T$ [20], where i_D is the linearized diffusive mass flux arising from concentration gradients, barodiffusion and electrodiffusion, and μ is the ion electrochemical potential. The associated thermal energy arising after shock front passage can be estimated as $Q = N_i \tau_i \bar{m}_i \tilde{D} |\nabla \mu|^2 / \partial_\alpha \mu|_{T,P,\Phi}$, where τ_s is the transit time for the shock front, \bar{m}_i is the mean ion mass, \tilde{D} is the ion diffusion coefficient [6], $\partial_\alpha \mu|_{T,P,\Phi} = (k_B T / m_D) / [\alpha(1-\alpha)(1 + \alpha(m_T / m_D - 1))]$, and Φ is the electrostatic potential. For the NIF CH-ablator ignition design with its signature four shocks [12], evaluation of Q in the DT ice layer gives nearly 30 J of anomalous heating from the effects of species separation. According to RH simulations of the maximum tolerable amount of fuel preheat from passage of the four shocks (or generated at late time from hohlraum Au M-band x rays or hot electrons) through the main fuel layer is nearly 100 J. Thus, one effect of transient species separation across the shock front is a possibly significant reduction in ignition performance margin.

In summary, thermodynamic arguments are used to show that an ablating mixed-species shell leads to an energy loss in the process of separating the constituent ions. This result is consistent with a calculated reduction in rocket ablation efficiency. A further effect of species separation is the reduced mass-ablation rate in a converging geometry. Direct evidence is provided for significant species separation based on Thomson scattering measurements of a direct-drive CH₂ planar sample. The main conclusion of this article is that mainline (single) fluid-based simulation techniques currently neglect species separation phenomena, thereby requiring

adaptations of these standard RH tools, use of multi-fluid PIC simulation techniques, or the simplifying option of single-species ablators, e.g., HDC or Al. Species separation effects in mixed-species fuels such as DT may also be important, requiring a more detailed assessment with PIC tools and remedial measures such as non-equimolar fuel concentrations and the use of weaker shocks to drive the implosion.

Useful discussions with Siegfried Glenzer are gratefully acknowledged. This work was performed under the auspices of Lawrence Livermore National Security, LLC (LLNS) under Contract DE-AC52-07NA27344 and supported by LDRD-11-ERD-075.

FIGURE CAPTIONS

Fig. 1: Fractional decrease in rocket efficiency versus hydrogen number fraction in CH ablator for various ionization states of carbon based on Eq. (1). Vertical dashed line denotes initial composition of CH ablator.

Fig. 2: Simulated 5 μm thick CH payload velocity versus time driven by 1ns 200 eV temperature source acting on fully mixed CH ablator (green) and segregated H + C layers (blue) where thickness of H layers is 1 μm and total thickness of ablator is 91.2 μm .

Fig. 3: Schematic of fully mixed C and H sample (left) and partially mixed sample (right) for calculating change in thermodynamic potential [Eq. 3].

Fig. 4: Separation energy versus hydrogen concentration for carbon ionization state of 6 (black), 5 (green) and 4 (blue) according to Eq. 3.

Fig. 5: Calculated hydrogen mass fraction (green) and number fraction (blue) versus radius for a NIF ignition CH ablator capsule [see Ref. 6] just after 4th shock launch based on Eq. 5, using $\alpha' \approx 0$ and $v_H - v \approx \delta = 87 \mu\text{m/ns}$ at leading edge of ablation front.

Fig. 6: Inferred hydrogen number fraction from Thomson scattering measurements 4 mm in front of CH₂ sample versus time relative to start of laser pulse (1ns flattop).

Fig. 7: Estimated energy invested in separating D and T ions in a NIF-scale implosion with 4.07×10^{19} ions and a mass-weighted ion temperature at the onset of hot-spot ignition.

REFERENCES

- [1] JD Lindl and EI Moses 2011 *Phys. Plasmas* **18** 050901
- [2] D Hicks *et al.* 2012 *Phys. Plasmas* **19** 122702
- [3] N Meezan *et al.* 2013 *Phys. Plasmas* **20** 056311
- [4] P Amendt *et al.* 2010 *Phys. Rev. Lett.* **105**, 115005
P Amendt *et al.* 2011 *Phys. Plasmas* **18**, 056308
- [5] P Amendt, C Bellei and SC Wilks 2012 *Phys. Rev. Lett.* **109** 075002
- [6] G Kagan and X-Z Tang 2012 *Phys. Plasmas* **19** 082709
- [7] G Kagan and X-Z Tang 2012 *Phys. Rev. Lett.* **19** 269501
- [8] P Amendt, C Bellei and SC Wilks 2012 *Phys. Rev. Lett.* **109** 269502
- [9] LD Landau and EM Lifshitz 1958 *Statistical Physics* (Oxford: Pergamon), p. 282
- [10] JS Ross, H-S Park, P Amendt, L Divol, NL Kugland, W Rozmus and SH Glenzer 2012 *Rev. Sci. Instrum.* **83** E323
- [11] PW Rambo and RJ Procassini 1995 *Phys. Plasmas* **2** 3130
DR Welch, DV Rose, BV Oliver and RE Clark 2001 *Nucl. Instrum. Methods Phys. Res. A* **464** 134
O Larroche 2003 *Eur. Phys. J. D* **27** 131
- [12] SW Haan *et al.* 2011 *Phys. Plasmas* **18** 051001
- [13] S Atzeni and J Meyer-ter-Vehn 2004 *The Physics of Inertial Fusion* (Oxford: Oxford Univ. Press), p. 233
- [14] G Gregori *et al.* 2006 *J. Quant. Spectrosc. Radiat. Transfer* **99** 225
- [15] O Jones *et al.* 2012 *Phys. Plasmas* **19** 056315
- [16] JD Lindl *Inertial Confinement Fusion* 1998 (New York: Springer), p. 55
- [17] TR Boehly *et al.* 1997 *Opt. Commun.* **133** 495
- [18] JA Fejer 1961 *Can. J. Phys.* **39**, 716
DE Evans 1970 *Plasma Phys.* **12** 573
- [19] D Casey *et al.* 2012 *Phys. Rev. Lett.* **108** 075002
- [20] LD Landau and EM Lifshitz 1959 *Fluid Mechanics* (Oxford: Pergamon)

Fig. 1

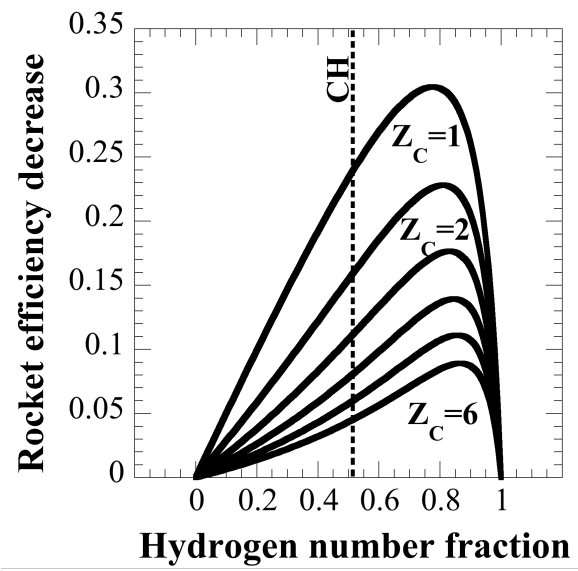


Fig. 2

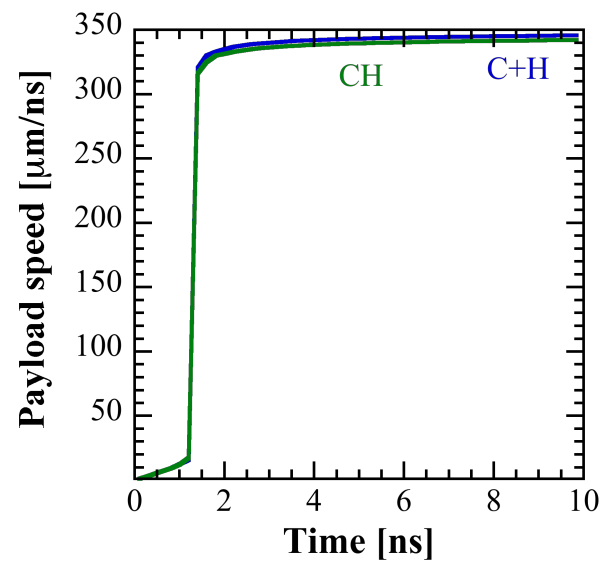


Fig. 3

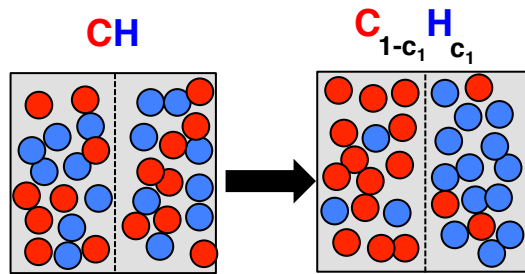


Fig. 4

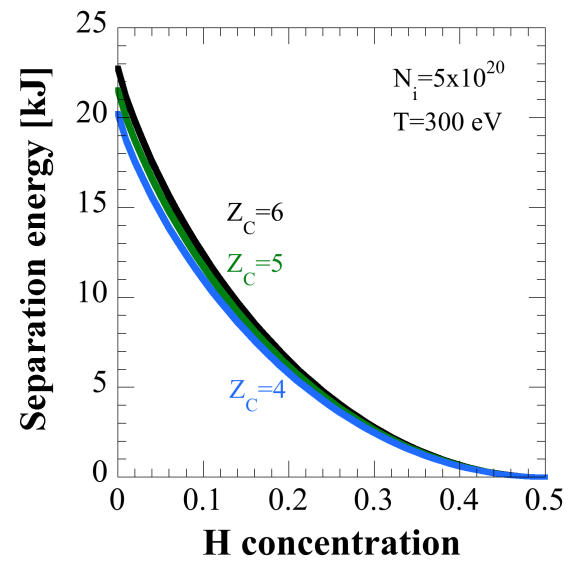


Fig. 5

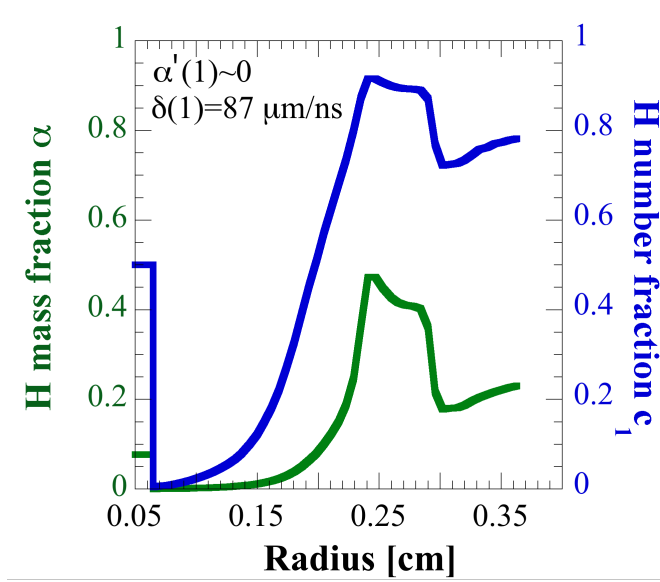


Fig. 6

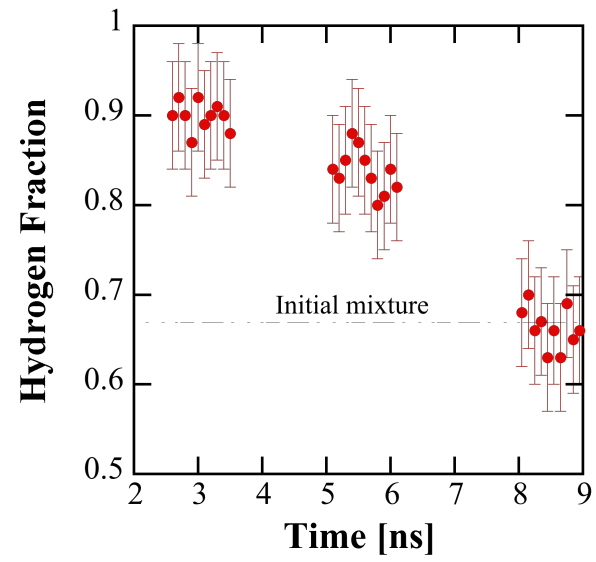


Fig. 7

